JACS
JOURNAL OF THE AMERICAN CHEMICAL SOCIETY
Communication
pubs.acs.org/JACS

Surface-Dependent, Ligand-Mediated Photochemical Etching of CdSe Nanoplatelets

Sung Jun Lim, Wonjung Kim, and Seung Koo Shin*

Bio-Nanotechnology Center, Department of Chemistry, Pohang University of Science and Technology, San 31, Hyoja-dong, Nam-gu, Pohang, Kyungbuk 790-784, Korea

Supporting Information

ABSTRACT: Photochemical etching of CdSe nanoplatelets was studied to establish a relationship between the nanocrystal surface and the photochemical activity of an exciton. Nanoplatelets were synthesized in a mixture of octylamine and oleylamine for the wurtzite (W) lattice or in octadecene containing oleic acid for the zinc-blende (ZB) lattice. For photochemical etching, nanoplatelets were dispersed in chloroform containing oleylamine and tributylphosphine in the absence or presence of oleic acid and then irradiated with light at the band-edge absorption maxima. Etching phenomena were characterized using UV−vis absorption spectroscopy and transmission electron microscopy. The absorption spectra of both W and ZB CdSe nanoplatelets showed that the exciton was confined in one dimension along the thickness. However, the two nanoplatelets presented different etching kinetics and erosion patterns. The rate of etching for W CdSe nanoplatelets was much faster than that for ZB nanoplatelets. Small holes were uniformly perforated on the planar surface of W nanoplatelets, whereas the corners and edges of ZB nanoplatelets were massively eroded without a significant perforation on the planar surface. This suggests that the amine-passivated surface of trivalent cadmium atoms on CdSe nanoplatelets is photochemically active, but the carboxylate-passivated surface of divalent cadmium atoms is not. Hence, the ligand, which induces the growth of W or ZB CdSe nanoplatelets, mediates the surface-dependent photochemical etching. This result implies that an electron−hole pair can be extracted from the planar surface of amine-passivated W nanoplatelets but from the corners and edges of carboxylate-passivated ZB nanoplatelets.

Nanocrystals exhibit novel photophysical and photochemical properties because of the confined surface boundary and the high surface-to-volume ratio.[1] For colloidal semiconductor nanocrystals, both the chemical composition of surface atoms and the type of surface ligands determine the lattice structure,[2,3] solubility,[4−6] surface reactivity,[5,6] and optoelectronic property.[7−9] The lattice structure is determined in the growth phase by a dynamic interplay between surface atoms and ligands, and the exciton activity is modulated by interactions between surface atoms and passivating ligands. We recently exploited such a surface−ligand interaction to passivate surface traps on CdSe nanocrystals with a binary amine−phosphine ligand system, which increases the radiative recombination rate of exciton.[8] Amine coordinates Cd dangling bonds on the surface, while phosphine passivates Se dangling bonds. This ligand system has also been used to assist the photochemical etching of nanocrystals such as quantum dots, nanorods, nanowires, and tetrapods, enabling precise control of the quantum-confinement size.[10] However, because surfaces of these nanocrystals are multifaceted, it is not well understood how the ligand affects the photochemical exciton activity on the individual surface plane of semiconductor nanocrystals.

To better understand the effects of ligands on the surface-dependent exciton activity, we studied the photochemical etching of wurtzite (W) and zinc-blende (ZB) CdSe nanoplatelets. Nanoplatelets afford well-defined surface planes that serve as the quantum-confinement boundary.[11−14] As shown in Scheme 1 (top), the terrace surfaces of W and ZB nanoplatelets are the $(110)_W$ plane perpendicular to the $[110]_W$ axis[11] and the $(100)_{ZB}$ plane perpendicular to the $[100]_{ZB}$ axis.[12−14] The $(110)_W$ plane is composed of trivalent Cd and Se atoms, whereas the $(100)_{ZB}$ plane is made up of either divalent Cd or divalent Se atoms. W and ZB nanoplatelets prepared by the literature methods are passivated with primary amines and fatty acid carboxylates, respectively. Monodentate amines (RNH_2) can coordinate trivalent Cd atoms on the $(110)_W$ surface to fulfill the tetravalency of the Cd atom, whereas bidentate carboxylates ($RCOO^-$) can chelate divalent Cd atoms on the $(100)_{ZB}$ surface, as illustrated in Scheme 1. Thus, the two

Scheme 1. Structure and Ligand Associated with Wurtzite and Zinc-Blende CdSe Nanoplatelets[a]

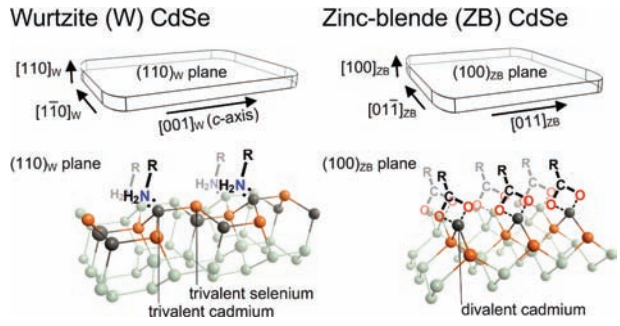

[a]Selenium atoms, orange; cadmium atoms, black.

Received: December 31, 2011
Published: April 27, 2012

   dx.doi.org/10.1021/ja212205q | J. Am. Chem. Soc. 2012, 134, 7576−7579

different surfaces on W and ZB CdSe nanoplatelet allow the study of surface- and ligand-dependent photochemical exciton activity confined along the thickness of nanoplatelets.

Briefly, we synthesized W and ZB nanoplatelets by following the literature methods[11,12] and confirmed their lattice structures by powder X-ray diffraction (XRD). For photochemical etching, nanoplatelets were dispersed in chloroform containing oleylamine (OLA) and tributylphosphine (TBP) in the presence or absence of oleic acid, and then irradiated with light from a pulsed laser. Optical and structural properties of nanoplatelets were monitored before and after photochemical etching using UV−vis absorption spectroscopy and transmission electron microscopy (TEM). The etched solution was characterized with NMR spectroscopy. See the Supporting Information for experimental details.

Major results are as follows: In the early stage of photochemical etching, the absorbance gradually decreased with little or no spectral shift for both W and ZB nanoplatelets, indicating a reduction in absorption cross-section without a change in quantum-confinement size. However, the two nanoplatelets displayed remarkably different erosion patterns resulting from dissimilar etching kinetics. TEM images showed that there were small holes uniformly perforated on the planar $(110)_W$ surface of W CdSe nanoplatelets, in comparison to massive erosions of edges and corners of ZB CdSe nanoplatelets with a little perforation on the planar $(100)_{ZB}$ surface. Moreover, the initial rate of photochemical etching of W CdSe nanoplatelets was much faster than that of ZB nanoplatelets. Evidently, the photochemical etching of nanoplatelets was surface-dependent, and the photochemical exciton activity was mediated by the ligand coordinated on the surface.

In more detail, W CdSe nanoplatelets were synthesized by reacting Se powder with the cadmium chloride−diamine complex, $CdCl_2(RNH_2)_2$, in a 1:1 octylamine/OLA (v/v) mixture.[11] ZB CdSe nanoplatelets were grown in 1-octadecene containing cadmium acetate, Se powder, and oleic acid.[12] Both syntheses used Cd salts and Se powder as the CdSe precursor. Importantly, both the ligand and the Cd/Se precursor ratio determined the lattice structure: Primary amine with a 1:3 Cd/Se ratio resulted in the W lattice, whereas fatty acid with a 2:1 Cd/Se ratio yielded the ZB lattice. The absorption spectra, TEM images, and XRD patterns of W and ZB CdSe nanoplatelets are displayed in Figure 1. The absorption spectra (Figure 1a) showed two characteristic peaks, the lowest energy light hole−electron and heavy hole−electron transitions, respectively, at 425 and 452 nm for W CdSe, respectively, and at 435 and 463 nm for ZB CdSe, respectively. The band-edge absorption wavelengths suggest an average thickness of 1.4 and 1.9 nm for W[11] and ZB[12] nanoplatelets, respectively. TEM images (Figure 1a, insets) displayed shapes of W (80 nm × 40 nm) and ZB (75 nm × 50 nm) nanoplatelets. XRD patterns (Figure 1b) were in line with bulk W and ZB lattice structures. Notably, all diffraction peaks were slightly shifted to larger angles for W nanoplatelets and to smaller angles for ZB nanoplatelets with respect to the bulk lattice, indicating contraction (1.5−6.3%) and expansion (0.9−2.3%) of the W and ZB lattice, respectively. Such a lattice reconstruction is considered to be due to a compressive stress on the $(110)_W$ surface by coordinated monodentate amines[15] in comparison to a tensile stress on the $(100)_{ZB}$ surface by chelated bidentate carboxylates.[16]

In the photochemical etching, chloroform was used as the solvent as well as a source of the reactive chloride ion.[10] We

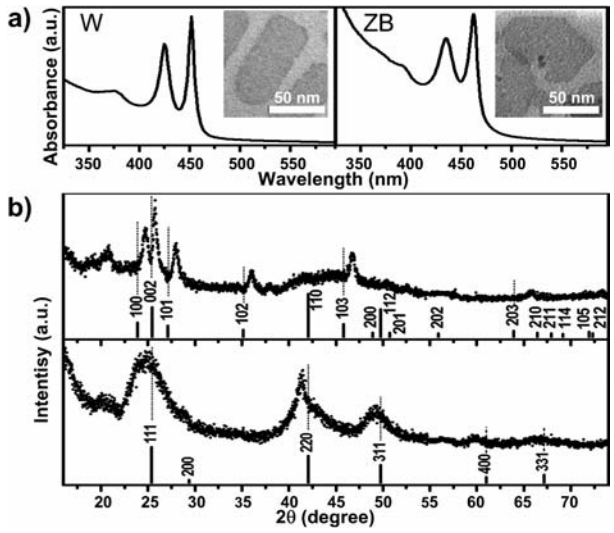

Figure 1. (a) Absorption spectra and TEM images (insets) of W and ZB CdSe nanoplatelets. (b) XRD patterns of W (top) and ZB (bottom) CdSe nanoplatelets. Vertical lines represent diffraction patterns of the bulk lattice.

have previously shown that the chloride ion is generated by photoinduced electron transfer from nanocrystals to chloroform adsorbed on the nanocrystal surface.[10] In non-chlorine-containing solvent, such as toluene, no photochemical etching was observed (see Figure S1). OLA and TBP were added to facilitate the etching, as they were known to dissolve $CdCl_2$ and Se into chloroform, respectively.[8,10] In the absence of OLA, nanoplatelets under photoirradiation were aggregated because the chloride layer formed on the surface decreased the solubility.[17] In the case of ZB CdSe nanoplatelets, oleic acid was added to prevent nanoplatelets from aggregating. Without oleic acid, a significant red-shift in the absorption spectra was observed with a spectral broadening and a baseline rise (see Figure S2), indicating the aggregation of ZB nanoplatelets. Meanwhile, W CdSe nanoplatelets did not aggregate in chloroform containing both OLA and TBP, regardless of the absence or presence of oleic acid. The addition of OLA and TBP to W CdSe nanoplatelets induced a blue-shift in the absorption peak by 1−2 nm, whereas that of OLA, TBP, and oleic acid to ZB CdSe nanoplatelets induced no shift. The photochemical etching was initiated by irradiating the etching solutions of W and ZB CdSe nanoplatelets with photons at their band-edge absorption maxima (λ_{abs}), 450 and 463 nm, respectively.

The absorption spectra and TEM images before and after the etching are compared in Figures 2 and 3 for W and ZB nanoplatelets, respectively. In the case of W CdSe nanoplatelets (Figure 2), photoirradiation induced a little peak shift in the absorption spectra. The absorbance was gradually reduced by one-third in 3 min and two-thirds in 20 min, indicating a reduction in absorption cross-section without a change in thickness. During 100 min photoirradiation at 450 nm, the absorption spectra continuously moved to shorter wavelength until the absorbance at 450 nm became zero, suggesting a significant reduction in quantum-confinement size of nanoplatelets. Increasing the laser fluence from 0.5 to 2 mJ cm^{-2} led to a much faster decrease in absorbance with a prominent rise in baseline, indicating the aggregation of nanoplatelets (Figure S3). Such a power-dependent aggregation is suggestive of the

dx.doi.org/10.1021/ja212205q | J. Am. Chem. Soc. 2012, 134, 7576−7579

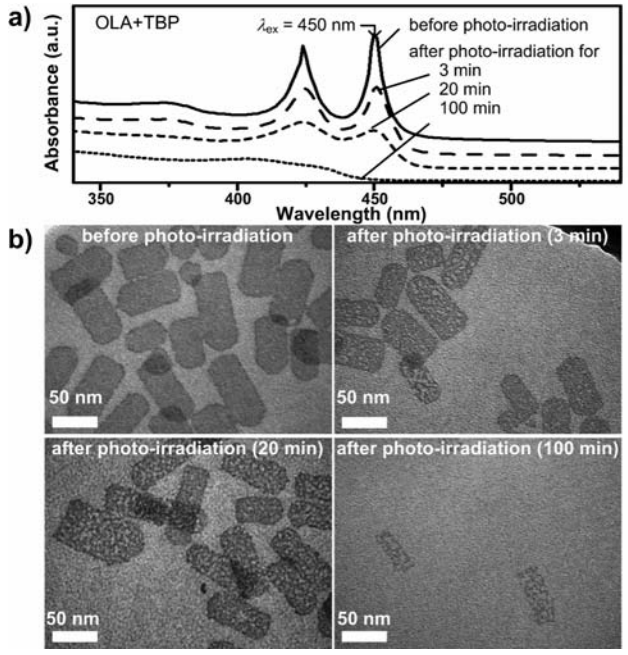

Figure 2. Absorption spectra (a) and TEM images (b) of W CdSe nanoplatelets before and after photochemical etching in chloroform containing OLA and TBP. λ_{ex} = 450 nm. The laser fluence per pulse was 0.5 mJ cm^{-2}.

heating effect[18] that promotes desorption of weakly bound primary amines from the W nanoplatelet surface. Changes in the morphology of nanoplatelets were apparent in TEM images taken before and after etching. After 3 min of photoirradiation, small holes were randomly perforated over the planar surface without a noticeable change in shape (see Figure S4a for more TEM images). These results suggest that the photochemical etching uniformly takes place on the $(110)_W$ surface. After 20 min of photoirradiation, the size of holes grew without a significant change in shape. However, the shape of nanoplatelets changed after 100 min of photoirradiation: The average size (length × width) was reduced from 80 nm × 40 nm before etching to 50 nm × 20 nm after etching. Similar changes in the optical spectra and surface erosion patterns were also observed from the photochemical etching of thicker W CdSe nanoplatelets at λ_{ex} = 580 nm (see Figure S5). Interestingly, addition of oleic acid to the etching solution containing both OLA and TBP decreased the etching rate by a factor of 2−3; however, changes in morphology of W CdSe nanoplatelets (see Figure S6) were almost identical to those of nanoplatelets etched in the absence of oleic acid (Figure 2).

The photochemical etching of ZB CdSe nanoplatelets took a longer time than that of W nanoplatelets, even though the laser fluence was increased 5 times from 0.5 to 2.5 mJ cm^{-2}. Photoirradiation led to a gradual decrease in the absorbance without any peak shifts: decreases of one-third in 30 min, two-thirds in 60 min, and nine-tenths in 90 min (Figure 3a). Although W nanoplatelets were significantly aggregated above the laser fluence of 1 mJ cm^{-2}, no aggregation of ZB nanoplatelets was observed at 2.5 mJ cm^{-2}. If electron transfer from nanoplatelets to chloroform did not occur, photons absorbed by nanoplatelets would have resulted in nonradiative heating because photoluminescence quantum yields of nanoplatelets were almost zero in chloroform. This surface heating could affect the stability of the ligand. Strongly bound

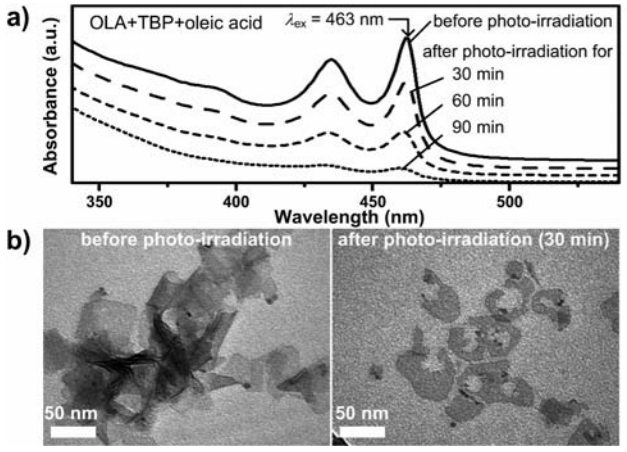

Figure 3. Absorption spectra (a) and TEM images (b) of ZB CdSe nanoplatelets before and after photochemical etching in chloroform containing OLA, TBP, and oleic acid. λ_{ex} = 463 nm. The laser fluence per pulse was 2.5 mJ cm^{-2}.

carboxylate might be more resistant to desorption than weakly bound primary amine. Similarly to W nanoplatelets, the absorption cross-section of ZB nanoplatelets decreased during photoirradiation. However, unlike W nanoplatelets, absorption peaks showed no shift after 90 min of photoirradiation and eventually disappeared without a trace, indicating that the nanoplatelet thickness remained unchanged during the entire etching period. TEM images in Figure 3b display the morphology of nanoplatelets before and after etching. After 30 min of photoirradiation, the edges and corners of ZB nanoplatelets were eroded and one large hole was perforated on average (see Figure S4b for more TEM images). Some ZB nanoplatelets showed holes even before the etching. After 60 and 90 min of photoirradiation, we were unable to take TEM images because of difficulties in purification of etched nanoplatelets. These results suggest that the etching mostly occurs from the edges on both the outer periphery and circumferential surfaces of inner holes of ZB CdSe nanoplatelets but not from the $(100)_{ZB}$ surface.

Based on our data, we propose a mechanism of surface-dependent, ligand-mediated photochemical etching of CdSe nanoplatelets (Scheme 2). The $(110)_W$ surface of W CdSe nanoplatelets is terminated with trivalent Cd atoms that are passivated with primary amines (RNH_2),[19] whereas the $(100)_{ZB}$ surface of ZB CdSe nanoplatelets is terminated with divalent

Scheme 2. Photochemical Etching of Wurtzite and Zinc-Blende CdSe Nanoplatelets in Chloroform

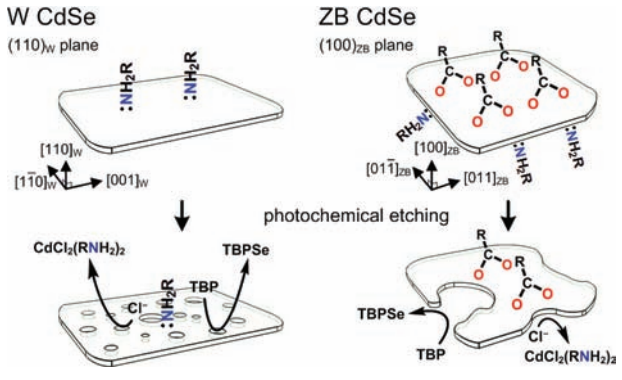

dx.doi.org/10.1021/ja212205q | J. Am. Chem. Soc. 2012, 134, 7576−7579

Cd atoms that are passivated with fatty acid carboxylates ($RCOO^-$). Photochemical etching is initiated by absorption of photons at the band-edge absorption maximum. Photoinduced electron transfer occurs from the conduction band of nanoplatelet to the lowest unoccupied molecular orbital of chloroform adsorbed on the surface to yield the reactive chloride ion.[10] The chloride ion removes Cd atoms on the surface, and then TBP removes coordinately unsaturated Se atoms. These sequential etching processes occur in a cyclic fashion. In the case of W CdSe nanoplatelets (Scheme 2, left), coordination of monodentate amine to the trivalent Cd atom is weak and labile;[20] thus the $(110)_W$ surface is easily accessible to chloroform and the chloride ion can react with Cd atoms on the surface to form cadmium chloride. Primary amine dissolves cadmium chloride into chloroform as $CdCl_2(RNH_2)_2$.[10] Meanwhile, holes left behind in the valence band of nanoplatelets can be transferred to Se atoms on the surface, and the oxidized Se atom is sequestered by TBP as TBPSe, which is soluble in chloroform.[8,10] ^{31}P NMR spectra (Figure S7) provide direct evidence for TBPSe, and ^1H NMR spectra (Figure S8) are in line with coordination of primary amines to $CdCl_2$ after etching. For ZB CdSe nanoplatelets (Scheme 2, right), coordination of bidentate carboxylate to the divalent Cd atom is strong and not labile;[16,21] thus, the $(100)_{ZB}$ surface buried under fatty acid carboxylates is rarely accessible to chloroform, and the monodentate chloride ion hardly replaces the bidentate carboxylate ligand on the surface. Instead, the chloride ion generated near the edges and corners of ZB nanoplatelets reacts with coordinatively unsaturated Cd atoms on the surface. Dissolution of Se atoms by TBP also takes place near the edges and corners because the $(100)_{ZB}$ surface is primarily covered with carboxylate-passivated Cd atoms without dangling Se atoms. Hence, the photochemical etching process is highly efficient on the amine-passivated surface but inefficient on the carboxylate-passivated surface. In comparison, the etching rate of bulk ZB CdSe semiconductor has been reported to be higher on the crystal facets with more surface dangling bonds,[22] such as the $(100)_{ZB}$ surface, contrary to our observation.

In conclusion, the ligand, which induces the growth of W or ZB CdSe nanoplatelets, mediates the photochemical etching of nanoplatelets. For both W and ZB CdSe nanoplatelets, the exciton is confined along the thickness of platelets. However, the two nanoplatelets show remarkably different erosion patterns resulting from different etching kinetics. Small holes are uniformly perforated on the planar $(110)_W$ surface of W CdSe nanoplatelets, whereas the edges and corners of ZB CdSe nanoplatelets are massively eroded with a little perforation on the planar $(100)_{ZB}$ surface. This result implies that the electron–hole pair can be extracted from the amine-passivated surface of CdSe nanoplatelets but not from the carboxylate-passivated surface. Moreover, the W CdSe nanoplatelet offers a larger surface area than the ZB CdSe nanoplatelet for photochemical conversion of exciton.

■ ASSOCIATED CONTENT

Supporting Information

Materials and syntheses, solvent-dependent etching, ligand-dependent stability, power-dependent etching, TEM images, etching of thick W CdSe nanoplatelets, NMR spectra, and estimated temperature jump. This material is available free of charge via the Internet at http://pubs.acs.org.

■ AUTHOR INFORMATION

Corresponding Author

skshin@postech.ac.kr

Notes

The authors declare no competing financial interest.

■ ACKNOWLEDGMENTS

S.J.L. acknowledges the postdoctoral support from the Brain Korea 21 program administered by the Ministry of Education, Science and Technology (MEST). We are thankful for the support from the National Research Foundation of Korea (Grant No. 2010-0019151) funded by MEST and the Advanced Scientific Analysis Instruments Development Project administered by the Korean Research Institute of Standards and Science.

■ REFERENCES

(1) Smith, A. M.; Nie, S. *Acc. Chem. Res.* **2010**, *43*, 190.
(2) Kumar, S.; Nann, T. *Small* **2006**, *2*, 316.
(3) Mahler, B.; Lequeux, N.; Dubertret, B. *J. Am. Chem. Soc.* **2010**, *132*, 953.
(4) Smith, A. M.; Duan, H.; Rhyner, M. N.; Ruan, G.; Nie, S. *Phys. Chem. Chem. Phys.* **2006**, *8*, 3895.
(5) Kim, Y.; Kim, W.; Yoon, H.-J.; Shin, S. K. *Bioconjugate Chem.* **2010**, *21*, 1305.
(6) Rosenthal, S. J.; Chang, J. C.; Kovtun, O.; McBride, J. R.; Tomlinson, I. D. *Chem. Biol.* **2011**, *18*, 10.
(7) Kim, Y.; Song, N. W.; Yu, H.; Moon, D. W.; Lim, S. J.; Kim, W.; Yoon, H.-J.; Shin, S. K. *Phys. Chem. Chem. Phys.* **2009**, *11*, 3497.
(8) Kim, W.; Lim, S. J.; Jung, S.; Shin, S. K. *J. Phys. Chem. C* **2010**, *114*, 1539.
(9) Hillhouse, H. W.; Beard, M. C. *Curr. Opin. Colloid Interface Sci.* **2009**, *14*, 245.
(10) Lim, S. J.; Kim, W.; Jung, S.; Seo, J.; Shin, S. K. *Chem. Mater.* **2011**, *23*, 5029.
(11) Son, J. S.; Wen, X.-D.; Joo, J.; Chae, J.; Baek, S.; Park, K.; Kim, J. H.; An, K.; Yu, J. H.; Kwon, S. G.; Choi, S.-H.; Wang, Z.; Kim, Y.-W.; Kuk, Y.; Hoffmann, R.; Hyeon, T. *Angew. Chem., Int. Ed.* **2009**, *48*, 6861.
(12) Ithurria, S.; Dubertret, B. *J. Am. Chem. Soc.* **2008**, *130*, 16504.
(13) Ithurria, S.; Bousquet, G.; Dubertret, B. *J. Am. Chem. Soc.* **2011**, *133*, 3070.
(14) Li, Z.; Peng, X. *J. Am. Chem. Soc.* **2011**, *133*, 6578.
(15) Meulenberg, R. W.; Jennings, T.; Strouse, G. F. *Phys. Rev. B* **2004**, *70*, 235311.
(16) Liu, H. *J. Phys. Chem. C* **2009**, *113*, 3116.
(17) Owen, J. S.; Park, J.; Trudeau, P.-E.; Alivisatos, A. P. *J. Am. Chem. Soc.* **2008**, *130*, 12279.
(18) If all photons were absorbed, the estimated temperature jump per laser pulse would be 2.8 and 12.6 K for W and ZB nanoplatelets, respectively (see Table S1).
(19) Although TOP used in the purification of W CdSe nanoplatelets contained a small amount of phosphonic acid (see Figure S9), which was known to bind strongly to CdSe nanocrystals (Morris-Cohen, A. J.; Donakowski, M. D.; Knowles, K. E.; Weiss, E. A. *J. Phys. Chem. C* **2010**, *114*, 897), this impurity did not play a significant role in the presence of excess primary amine (see Figure S10).
(20) Ji, X.; Copenhaver, D.; Sichmeller, C.; Peng, X. *J. Am. Chem. Soc.* **2008**, *130*, 5726.
(21) Kopping, J. T.; Patten, T. E. *J. Am. Chem. Soc.* **2008**, *130*, 5689.
(22) Seker, F.; Meeker, K.; Kuech, T. F.; Ellis, A. B. *Chem. Rev.* **2000**, *100*, 2505.